The Cr-Zr-Ca armalcolite in lunar rocks is loveringite: Constraints from electron backscatter diffraction measurements

Ai-Cheng Zhang[1,2,*], Run-Lian Pang[1,†], Naoya Sakamoto[3], and Hisayoshi Yurimoto[3,4,5]

[1]State Key Laboratory for Mineral Deposits Research, School of Earth Sciences and Engineering, Nanjing University, Nanjing 210023, China
[2]CAS Center for Excellence in Comparative Planetology, China
[3]Isotope Imaging Laboratory, Creative Research Institution, Hokkaido University, Sapporo 001-0021, Japan
[4]Department of Natural History Sciences, Hokkaido University, Sapporo 060-0810, Japan
[5]Institute of Space and Astronautical Science, Japan Aerospace Exploration Agency, Kanagawa 252-5210, Japan

Abstract

"Cr-Zr-Ca armalcolite" is a mineral originally found in Apollo samples five decades ago. However, no structural information has been obtained for this mineral. In this study, we report a new occurrence of "Cr-Zr-Ca armalcolite" and its associated mineral assemblage in an Mg-suite lithic clast (Clast-20) from the brecciated lunar meteorite Northwest Africa 8182. In this lithic clast, plagioclase (An = 88–91), pyroxene (Mg#[Mg/(Mg+Fe)] = 0.87–0.91) and olivine (Mg# = 0.86–0.87) are the major rock-forming minerals. Armalcolite and "Cr-Zr-Ca armalcolite" are observed with other minor phases including ilmenite, chromite, rutile, fluorapatite, merrillite, monazite, FeNi metal, and Fe-sulfide. Based on 38 oxygen atoms, the chemical formula of "Cr-Zr-Ca armalcolite" is $(Ca_{0.99}Na_{0.01})_{\Sigma1.00}(Ti_{14.22}Fe_{2.06}Cr_{2.01}Mg_{1.20}Zr_{0.54}Al_{0.49}Ca_{0.21}Y_{0.05}Mn_{0.04}Ce_{0.03}Si_{0.03}La_{0.01}Nd_{0.01}Dy_{0.01})_{\Sigma20.91}O_{38}$. Electron backscatter diffraction (EBSD) results reveal that the "Cr-Zr-Ca armalcolite" has a loveringite $R\overline{3}$ structure, differing from the armalcolite *Bbmm* structure. The estimated hexagonal cell parameters *a* and *c* of "Cr-Zr-Ca armalcolite" are 10.55 and 20.85 Å, respectively. These structural and compositional features indicate that "Cr-Zr-Ca armalcolite" is loveringite, not belonging to the armalcolite family. Comparison with "Cr-Zr-Ca armalcolite" and loveringite of other occurrences implies that loveringite might be an important carrier of rare earth elements in lunar Mg-suite rocks. The compositional features of plagioclase and mafic silicate minerals in Clast-20 differ from those in other Mg-suite lithic clasts from Apollo samples and lunar meteorites, indicating that Clast-20 represents a new example of diverse lunar Mg-suite lithic clasts.

Keywords: Loveringite, armalcolite, Cr-Zr-Ca armalcolite, monazite, Mg-suite lithic clast, NWA 8182, lunar meteorite, EBSD

Introduction

Five decades ago, Apollo astronauts collected precious samples from the surface of the Moon and brought them back to Earth. These samples are fundamental materials for understanding the origin and evolutionary history of the Moon (Heiken et al. 1991; Papike et al. 1998; Jolliff et al. 2006). In these Apollo samples, scientists found a new oxide mineral $(Mg,Fe)Ti_2O_5$ with orthorhombic *Bbmm* structure (Anderson et al. 1970). This phase was named armalcolite after the three astronauts (Neil A. Armstrong, Edwin E. Aldrin, and Michael Collins) of the Apollo 11 mission. At the same time, a phase that is similar chemically to armalcolite but contains a few weight percent of Cr_2O_3, ZrO_2, and CaO was also observed and termed "Cr-Zr-Ca armalcolite." The name "Cr-Zr-Ca armalcolite" has been used for five decades since its discovery (e.g., Steele and Smith 1972; Peckett et al. 1972; Haggerty 1972, 1973; Reid et al. 1973; Steele 1974; Treiman and Drake 1983; Treiman and Gross 2015).

"Cr-Zr-Ca armalcolite" was also described in terrestrial rocks (e.g., Haggerty 1983; Haggerty et al. 1983; Schulze 1990; Contini et al. 1993; Grégoire et al. 2000).

Armalcolite is an oxide mineral containing relatively small polyhedral sites for Mg, Fe, and Ti. In principle, cations with a large radius such as Ca^{2+} are not readily incorporated into the structure of armalcolite. This leads to a puzzle of whether "Cr-Zr-Ca armalcolite" belongs to the armalcolite family or not from the aspect of the crystal structure (Levy et al. 1972; Lattard 1987). This puzzle has triggered theoretical considerations on the potential structure of "Cr-Zr-Ca armalcolite" (Săbău and Alberico 2007). Săbău and Alberico (2007) suggested that "Cr-Zr-Ca armalcolite" might be loveringite ($R\overline{3}$) or a hexagonal phase ($P\overline{3}$) with a hypothetical structure intermediate between crichtonites and magnetoplumbites, based on their crystal-chemical consideration. However, due to small grain sizes, the "Cr-Zr-Ca armalcolite" that was described in the literature was not structurally characterized.

During a study of the brecciated lunar meteorite Northwest Africa (NWA) 8182, we observed the presence of both armalcolite and the so-called "Cr-Zr-Ca armalcolite" in an Mg-suite

* E-mail: aczhang@nju.edu.cn
† Present address: Institute of Geochemistry, Chinese Academy of Sciences, Guiyang 550081, China

lithic clast (Clast-20). Considering the advantage of the electron backscatter diffraction (EBSD) technique for phase identification at a micrometer scale, we obtained the structural information on the "Cr-Zr-Ca armalcolite." Based on the EBSD results and compositional features, the "Cr-Zr-Ca armalcolite" turns out to be loveringite, not belonging to the armalcolite family. Here we report the occurrence, mineral composition, structural identification of the "Cr-Zr-Ca armalcolite" phase, and potential significance to the lunar science.

ANALYTICAL METHODS

Petrographic texture of the NWA 8182 meteorite was observed using a JEOL 7000F field-emission scanning electron microscope (FE-SEM) at Hokkaido University, Japan and a Zeiss Supra 55 FE-SEM instrument at Nanjing University, China. Backscattered electron (BSE) images were made to record the petrographic textures. An energy-dispersive spectrometer (EDS), which was controlled by the Oxford Aztec Software, was used to obtain the qualitative compositions of minerals. Elemental mapping was performed to illustrate the distributions of elements in the lithic clast containing "Cr-Zr-Ca armalcolite."

Chemical compositions of most minerals in this study were measured using a JEOL 8100 electron probe microanalyzer (EPMA) with wavelength-dispersive spectrometers at Nanjing University. For rare earth elements in the Cr-Zr-Ca armalcolite, the JEOL 8530 field-emission gun EPMA instrument at the same laboratory was used. Both instruments were operated at an accelerating voltage of 15 kV and a focused beam of 20 nA. The elements were measured 20 s for peak and 10 s for the background. Natural and synthetic standards were used for concentration calibration. All data were reduced with the atomic number-absorption-fluorescence (ZAF) procedure installed in the JEOL EPMA instruments. Typical detection limits are better than 0.02 wt% for most elements and approximately 0.03 wt% for rare earth elements.

Structural characterizations of minerals in this study were carried out using an EBSD detector installed on the JEOL 7000F FE-SEM instrument at Hokkaido University. The sample was tilted 70° compared to the normal configuration and measured with an accelerating voltage of 20 kV and a beam current of 4 nA. The EBSD detector was controlled by the Oxford Aztec Software. Qualitative chemical composition and EBSD pattern were obtained simultaneously. Potential candidates from the data set of the software were chosen based on the constituent elements. A few candidates that are not included in the data set were also used by configuring parameter files based on the structural parameters from the *American Mineralogist Crystal Structure Database.* The Aztec software automatically suggests indexing solutions ranked by the lowest "mean angular deviation" (MAD) as an index of "goodness of fit." MAD numbers <1 are considered desirable for accurate solutions.

RESULTS

NWA 8182 is a brecciated lunar meteorite. It consists of abundant lithic clasts and mineral fragments (Fig. 1). Both feldspathic and basaltic clasts are present in NWA 8182, but the former is more abundant. Lithic clasts consisting mainly of silica and alkaline feldspar are also observed. The regions between lithic clasts and mineral fragments are glassy with abundant vesicles.

The lithic clast Clast-20 is a magnesian suite clast of approximately 1.3×0.7 mm in size, locating at the edge of the polished section (Fig. 1). It consists mainly of plagioclase (55.8 vol%), olivine (28.2 vol%), and pyroxene (14.4 vol%) (Fig. 2). The representative compositions of these silicate minerals are given in Table 1. The plagioclase (An = 88–91) in Clast-20 has
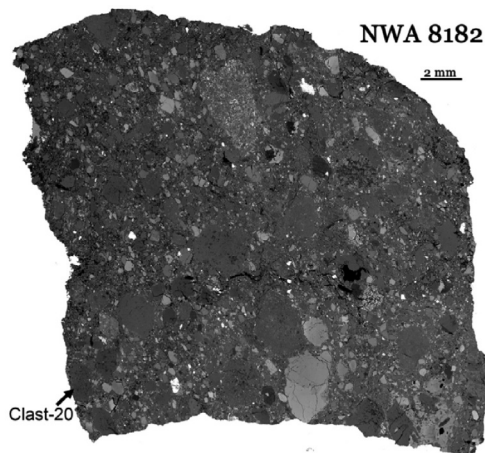

FIGURE 1. Mosaic backscattered electron image of the NWA 8182 lunar meteorite, which contains both feldspathic and basaltic breccias. The location of Clast-20 is indicated by the arrow in the lower left of the mosaic image.
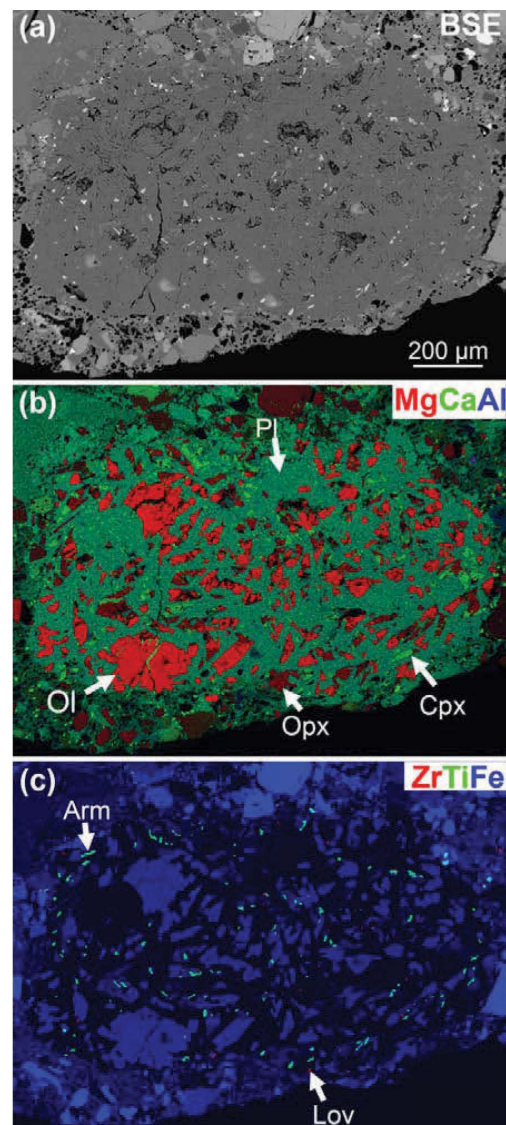

FIGURE 2. BSE image and false color images based on X-ray elemental mapping results of Clast-20 in NWA 8182. Ol = olivine; Opx = orthopyroxene; Cpx = high-Ca pyroxene; Pl = plagioclase; Arm = armalcolite; Lov = loveringite. (Color online.)
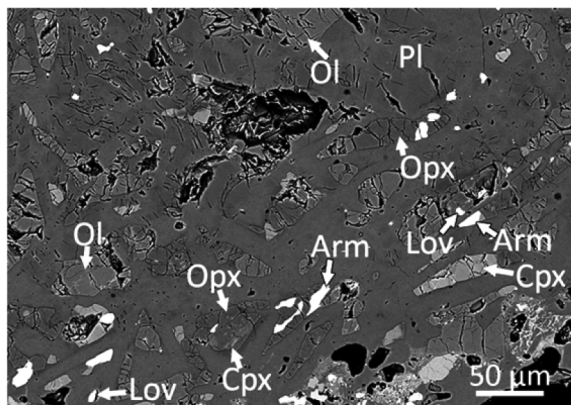
TABLE 1. Representative EPMA compositions of silicate minerals in Clast-20

	High-Ca pyroxene			Low-Ca pyroxene			Plagioclase		Olivine	
SiO_2	52.7	51.7	51.8	55.4	55.2	55.6	44.5	45.3	39.2	38.8
TiO_2	1.60	2.31	1.69	0.62	0.97	0.56	0.05	0.03	0.07	0.07
Al_2O_3	2.13	2.24	2.37	1.06	1.67	0.97	35.4	34.4	0.04	0.03
Cr_2O_3	0.52	0.32	0.60	0.40	0.57	0.32	0.03	0.02	bdl	bdl
MgO	17.2	17.8	17.1	32.1	31.3	32.5	0.07	0.08	47.2	46.8
FeO	3.18	3.98	3.11	8.69	8.45	8.52	0.18	0.22	13.2	13.7
MnO	0.08	0.11	0.11	0.18	0.16	0.17	bdl	0.02	0.17	0.19
CaO	22.2	20.9	22.6	1.31	1.63	1.47	18.2	18.3	0.08	0.11
Na_2O	0.14	0.19	0.15	bdl	bdl	bdl	0.94	1.34	bdl	bdl
K_2O	bdl	bdl	bdl	bdl	bdl	bdl	0.06	0.17	bdl	bdl
Total	99.75	99.55	99.53	99.76	99.95	100.1	99.43	99.88	99.96	99.70
Si	1.921	1.893	1.899	1.944	1.934	1.943	2.066	2.099	0.976	0.972
Ti	0.044	0.063	0.046	0.016	0.025	0.015	0.002	0.001	0.001	0.001
Al	0.091	0.097	0.102	0.044	0.069	0.040	1.935	1.875	0.001	0.001
Cr	0.015	0.009	0.017	0.011	0.016	0.009	0.001	0.001	bdl	bdl
Mg	0.939	0.979	0.940	1.689	1.643	1.705	0.005	0.005	1.764	1.760
Fe	0.096	0.121	0.095	0.254	0.246	0.248	0.007	0.008	0.273	0.286
Mn	0.002	0.003	0.003	0.005	0.005	0.005	bdl	0.001	0.004	0.004
Ca	0.868	0.818	0.887	0.049	0.061	0.055	0.904	0.906	0.002	0.003
Na	0.010	0.013	0.011	bdl	bdl	bdl	0.084	0.120	bdl	bdl
K	bdl	bdl	bdl	bdl	bdl	bdl	0.004	0.010	bdl	bdl
Cations	3.987	3.998	4.000	4.013	3.999	4.019	5.008	5.026	3.022	3.027
Mg#	0.91	0.89	0.91	0.87	0.87	0.87			0.87	0.86
Wo	45.6	42.6	46.2	2.5	3.1	2.7	An 91.1	87.5		
En	49.3	51.0	48.9	84.8	84.2	84.9	Ab 8.5	11.6		
Fs	5.1	6.3	4.9	12.7	12.6	12.4	Or 0.4	0.9		

Notes: Mg# = Mg/(Mg+Fe) in moles; bdl: below detection limit. Cations of pyroxene, plagioclase, and olivine are calculated based on 6, 8, and 4 oxygen atoms, respectively.

FIGURE 3. BSE image of a typical region in Clast-20. Mineral abbreviations are the same as those in Figure 2.

TABLE 2. EPMA compositions of ilmenite, chromite, and armalcolite in Clast-20

	Ilmenite	Chromite		Armalcolite				
SiO_2	0.10	0.06	0.41	0.47	0.09	0.14	0.08	0.11
TiO_2	55.6	0.56	1.19	71.9	72.8	73.5	72.5	72.3
ZrO_2	bdl	bdl	bdl	0.63	0.59	0.55	0.43	0.50
Al_2O_3	0.22	25.8	17.6	0.76	0.71	0.67	0.75	1.12
Cr_2O_3	0.79	42.7	48.8	1.75	1.70	0.95	0.86	1.95
MgO	10.9	10.7	9.46	11.3	10.8	10.9	10.5	10.9
FeO	31.2	19.7	21.5	11.5	12.3	12.4	13.7	11.8
MnO	0.36	0.22	0.32	0.10	0.10	0.08	0.05	0.10
CaO	0.59	0.33	0.56	0.62	0.53	0.35	0.53	0.64
Total	99.76	100.1	99.84	99.03	99.62	99.54	99.40	99.42
Si	0.002	0.002	0.013	0.017	0.003	0.005	0.003	0.004
Ti	0.975	0.013	0.029	1.924	1.945	1.961	1.949	1.931
Zr	bdl	bdl	bdl	0.011	0.010	0.010	0.008	0.009
Al	0.006	0.932	0.666	0.032	0.030	0.028	0.032	0.047
Cr	0.015	1.037	1.238	0.049	0.048	0.027	0.024	0.055
Mg	0.384	0.495	0.456	0.606	0.577	0.583	0.566	0.583
Fe	0.608	0.505	0.576	0.342	0.366	0.368	0.409	0.351
Mn	0.007	0.006	0.009	0.003	0.003	0.002	0.002	0.003
Ca	0.015	0.011	0.019	0.024	0.020	0.013	0.020	0.024
Cations	2.013	3.001	3.007	3.008	3.002	2.997	3.013	3.006
Mg#	0.39	0.50	0.44	0.64	0.61	0.61	0.58	0.62

Notes: Mg# = Mg/(Mg+Fe) in moles; bdl: below detection limit. Cations in ilmenite, chromite, and armalcolite are calculated based on 3, 4, and 5 oxygen atoms.

partly transformed into glass, with the untransformed regions containing abundant irregular fractures (Fig. 3). Olivine grains are anhedral to euhedral in shape with a grain size varying from 10 to 200 μm. These olivine grains have a very limited compositional range (Mg# = 0.86–0.87). Both orthopyroxene and clinopyroxene are observed with subhedral to euhedral shapes. Their compositions are $En_{84.2-84.9}Fs_{12.3-12.7}Wo_{2.5-3.1}$ (Mg# = 87) and $En_{48.8-51.0}Fs_{5.1-6.3}Wo_{42.6-46.2}$ (Mg# = 89–91), respectively. The orthopyroxene and clinopyroxene occur either as discrete grains or form an intergrowth texture with each other (Fig. 3). The grain sizes of pyroxene are usually smaller than those of olivine but could be up to 100 μm in length.

Accessory minerals (~1.6 vol%) in Clast-20 include various Ti-rich oxide minerals (~1 vol%, armalcolite, ilmenite, "Cr-Zr-Ca armalcolite," and rutile), chromite, phosphate minerals, FeNi metal, and Fe-sulfide. Compositions of these oxide minerals are given in Tables 2 and 3. Both armalcolite and "Cr-Zr-Ca armalcolite" are common in Clast-20. They mainly occur as discrete grains and are closely associated with olivine or pyroxene (Figs. 3–4). Some armalcolite grains occur as clean grains in BSE images; however, most of them contain tiny ilmenite inclusions (Figs. 4b and 4c). "Cr-Zr-Ca armalcolite" mainly occurs as clean grains and is brighter in BSE images than armalcolite (Fig. 4). Armalcolite in this study is dominated by TiO_2, MgO, and FeO with an Mg# value of 0.58–0.64. The Cr_2O_3, ZrO_2, and CaO contents of armalcolite are 0.86–1.95, 0.43–0.63, and 0.35–0.79 wt%, respectively (Table 2). The EBSD patterns of armalcolite can only be indexed with the pseudobrookite *Bbmm* structure (Fig. 5) based on the atomic coordinates of the synthetic $(Mg_{0.5}Fe_{0.5})Ti_2O_5$ (Wechsler 1977), with the mean angular deviations as low as 0.26. They cannot be indexed with the structures of other Ti-oxide phases.

The "Cr-Zr-Ca armalcolite" grains contain 67.5–69.7 wt% TiO_2. Their MgO and FeO contents (2.7–3.0 and 8.6–9.4 wt%, respectively; Mg# = 0.35–0.38) are lower than those in armalcolite (Tables 2 and 3). Instead, they contain distinctly higher contents of Cr_2O_3 (8.4–10.0 wt%), ZrO_2 (3.7–4.3 wt%), and CaO (4.3–4.2 wt%) than armalcolite (Table 3). The "Cr-Zr-Ca armalcolite" grains also contain minor rare earth elements (0.31–0.41 wt% Y_2O_3, 0.09–0.13 wt% La_2O_3, 0.21–0.39 wt% Ce_2O_3, 0.06–0.11 wt% Nd_2O_3, and 0.02–0.12 wt% Dy_2O_3). Although Pr, Sm, and Gd were also measured, their concentrations are below detection limits. The EBSD patterns of "Cr-Za-Ca armalcolite" can only be indexed with the loveringite $R\overline{3}$ structure (Fig. 6) based on the atomic coordinates from natural loveringite (Gatehouse et al. 1978), with the mean angular deviations as low as 0.22. They cannot be indexed with the structures of other Ti-rich oxide phases including magnetoplumbite. Based on the mean composition of four spot analyses (Table 3) and 38 oxygen atoms, the chemical formula of "Cr-Zr-Ca

TABLE 3. EPMA compositions of loveringite in Clast-20 and lunar "Cr-Zr-Ca armalcolite" and some loveringite in literature

	This study		Cr-Zr-Ca armalcolite																Loveringite		
			S72	S72	S72	L72	P72	R73	H73	H73	S74	H83	H83	H83	T15	T15	T15	C78	M13	M13
SiO₂	0.12	0.11	0.14	0.22	0.17	0.18	0.6	0.2	0.27	0.23	0.22	0.47	0.11	0.37	—	0	0	0	0	0.93	
TiO₂	69.68	67.47	68.90	67.2	67.7	67.9	70.1	68.8	65.42	66.52	66.49	68.58	61.4	62.8	62.2	71.77	70.11	69.81	60.31	59.28	59.14
ZrO₂	3.65	3.93	4.07	4.30	3.65	3.71	3.61	4.5	6.1	6.55	6.01	6.38	4.4	6	6.65	6.05	1.93	1.14	2.91	5.12	5.36
Al₂O₃	1.30	1.61	1.49	1.89	1.92	1.84	1.6	0.9	1.48	1.49	1.55	2.12	1.05	0.98	1.32	0.16	0.41	1.32	0.8	0.95	1.3
Cr₂O₃	8.40	10.03	9.77	8.24	7.83	7.78	8.8	4.3	7.67	10.31	11.48	9.67	10.6	10.1	10.1	5.29	7.91	6.07	6.48	12.17	0.15
Fe₂O₃						3.57			1.98	2.31	2.5	2.38					5.87	1.84	21.19	14.21	22.89
MgO	2.97	2.94	2.70	3.74	3.76	6.6	1.9	1.7	10.66	9.33	8.47	9.78	2.65	3.05	3.05	6.3	6.47	1.52	1.52	2.35	1.46
FeO	8.63	8.55	9.11	6.56	6.39	0.06	9	13.4	0.1	0.13	0.1	0.21	7.76	8.21	7.47	7.47	0.14				
MnO	0.16	0.18	0.18	0.08	0.05	3.02	0	0.2	3.4	3.4	3.49	3.72	0.09	0.08	0.11	0.11	4.38		0.21	0.27	0.11
CaO	4.21	4.08	3.98	3.36	3.07	0.05	3.1	3.1					3.19	3.18	4.31	4.31			2.51	2.54	3.23
Na₂O	0.03	0.00	0.03	0.04															0.06	0.06	0.15
K₂O	0.02	0.02	0.01																0.03	0.03	0.04
Y₂O₃	0.41	0.31	0.34											0.18	0.01				0.23	0.15	0.04
La₂O₃	0.13	0.18	0.09											0.08	0.05				0.93	1.26	0.11
Ce₂O₃	0.22	0.35	0.21												0.09				1.25	1.38	0.2
Nd₂O₃	0.09	0.11	0.06																0.26	0.23	0.01
Dy₂O₃	0.12	0.02	0.10																		
Nb₂O₅									0.37	0.45				1.14	2.13						
Total	100.2	99.88	100.9	99.98	94.98	94.65	94.56	99.6	98.7	97.53	100.1	101.1	93.77	94.25	94.82	98.74	98.71	98.6	98.66	100	95.12
Si	0.033	0.031	0.039	0.063	0.049	0.052	0.165	0.057	0.077	0.064	0.060	0.128	0.032	0.109	0.000	0.000	0.000	0.000	0.000	0.000	0.271
Ti	14.451	14.080	14.098	14.445	14.570	14.633	14.521	14.701	14.097	13.913	13.754	14.052	13.925	13.740	14.846	14.506	14.747	14.506	12.935	12.594	12.956
Zr	0.491	0.532	0.545	0.582	0.509	0.518	0.504	0.604	0.845	0.915	0.855	0.584	0.862	0.952	0.259	0.153	0.538	0.405	0.705	0.761
Al	0.422	0.526	0.488	0.637	0.647	0.621	0.519	0.301	0.500	0.488	0.502	0.681	0.365	0.339	0.052	0.133	0.437	0.269	0.316	0.446
Cr	1.831	2.200	2.145	1.861	1.771	1.762	1.916	0.966	1.737	2.266	2.496	2.082	2.470	2.345	1.150	1.720	1.348	1.461	2.717	0.035	1.406
Fe³⁺					0.028													4.546	3.020	5.016
Mg	1.220	1.216	1.118	1.593	1.603	1.524	0.780	0.720	0.845	0.957	1.025	0.966	1.234	1.335	2.582	2.406	0.770	0.646	0.989	0.634
Fe²⁺	1.990	1.983	2.116	1.568	1.529	1.581	2.072	3.183	2.553	2.169	1.948	2.228	2.067	2.016	1.718	1.488	2.656	0.000	0.000	0.000	3.165
Mn	0.037	0.042	0.042	0.019	0.012	0.015	0.000	0.048	0.024	0.031	0.023	0.048	0.022	0.020	0.026	0.033	0.048	0.051	0.065	0.027	0.168
Ca	1.243	1.213	1.184	1.029	0.941	0.927	0.915	0.943	1.043	1.013	1.028	1.086	1.007	1.000	1.270	1.291	1.194	0.767	0.769	1.008	1.100
Na	0.016	0.000	0.016	0.022	0.028														0.033	0.035	0.085
K	0.000	0.007	0.004																0.011	0.015
Y	0.060	0.046	0.050											0.018	0.001				0.023	0.006
La	0.013	0.018	0.009											0.008	0.005				0.035	0.131	0.012
Ce	0.022	0.036	0.021												0.009				0.098	0.143	0.021
Nd	0.009	0.011	0.006																0.130	0.023	0.001
Dy	0.011	0.002	0.009																0.026		
Nb									0.047	0.056				0.142	0.265						
Sum	21.849	21.942	21.927	21.745	21.668	21.619	21.492	21.764	21.792	21.715	21.691	21.855	21.762	21.857	21.927	21.745	21.780	21.389	21.537	21.293	21.965
Mg#	0.38	0.38	0.37	0.35	0.50	0.51	0.49	0.27	0.18	0.25	0.31	0.34	0.37	0.38	0.40	0.60	0.62	0.22	0.18	0.18	0.18

Notes: Mg# = Mg/(Mg+Fe) in moles. Data sources: S72 = Steele and Smith (1972); L72 = Levy et al. (1972); P72 = Peckett et al. (1972); R73 = Reid et al. (1973); H73 = Haggerty (1973); S74 = Steele (1974); R73 = Reid et al. (1973); H83 = Haggerty (1983); T15 = Treiman and Gross (2015); C78 = Campbell and Kelly (1978); M13 = Ma et al. (2013). Cations in this table are calculated based on 38 oxygen atoms.
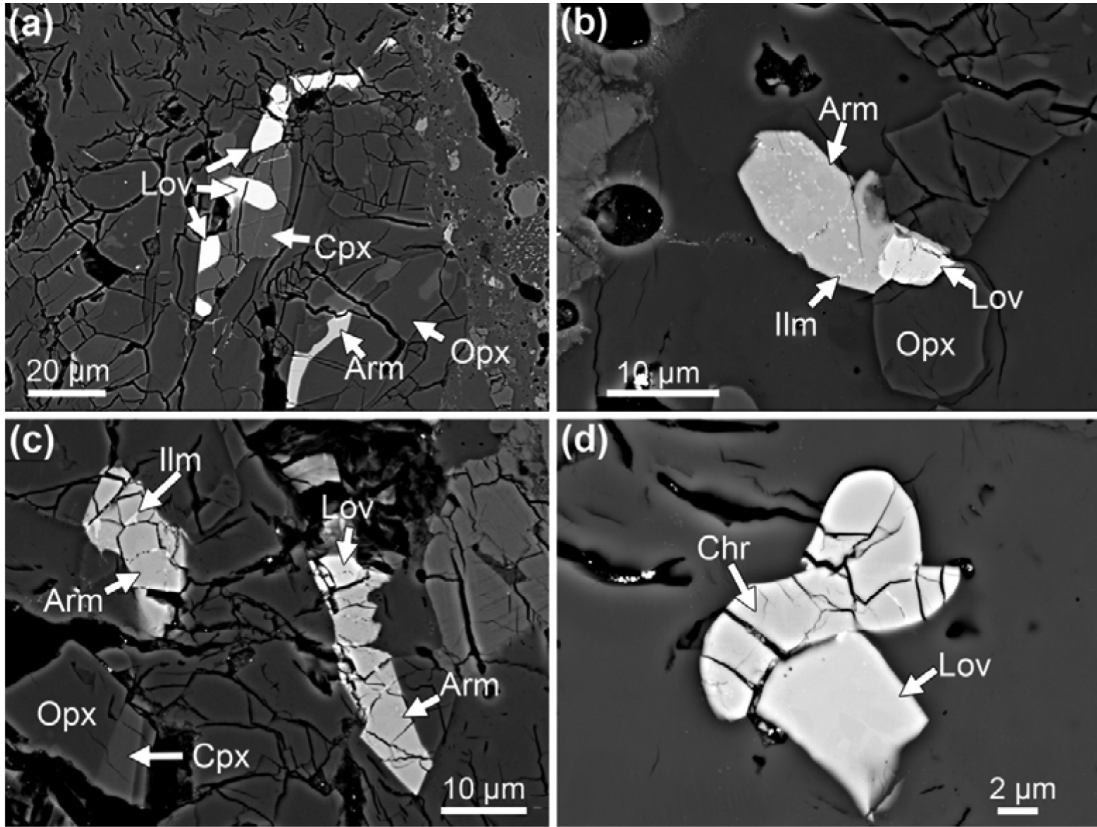
FIGURE 4. BSE images showing the intergrowth textures among loveringite, armalcolite, and chromite. Note that the armalcolite grain contains tiny grains of ilmenite. Ol = olivine; Opx = orthopyroxene; Cpx = high-Ca pyroxene; Pl = plagioclase; Arm = armalcolite; Lov = loveringite; Ilm = ilmenite; Chr = chromite.
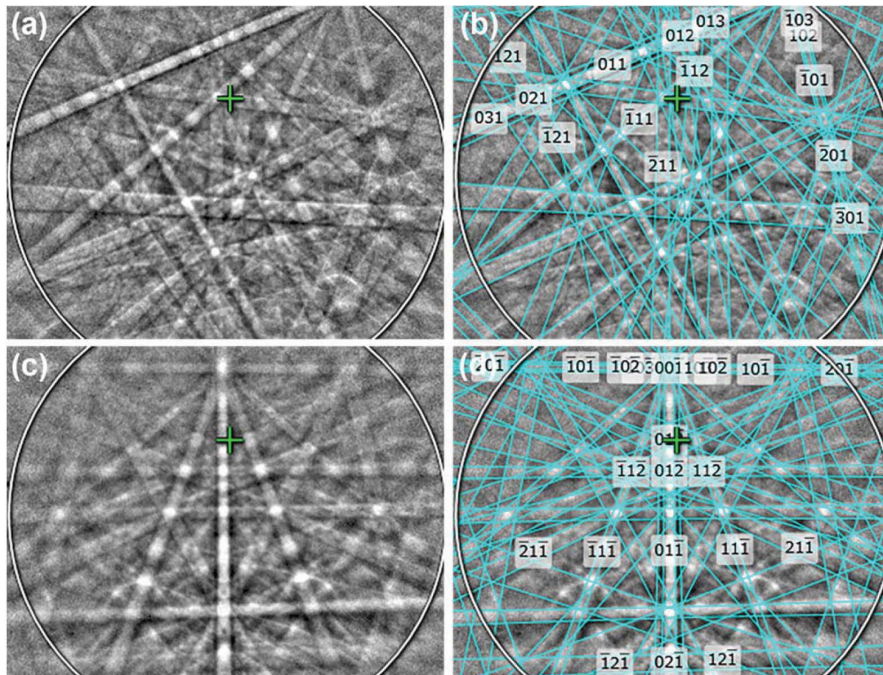

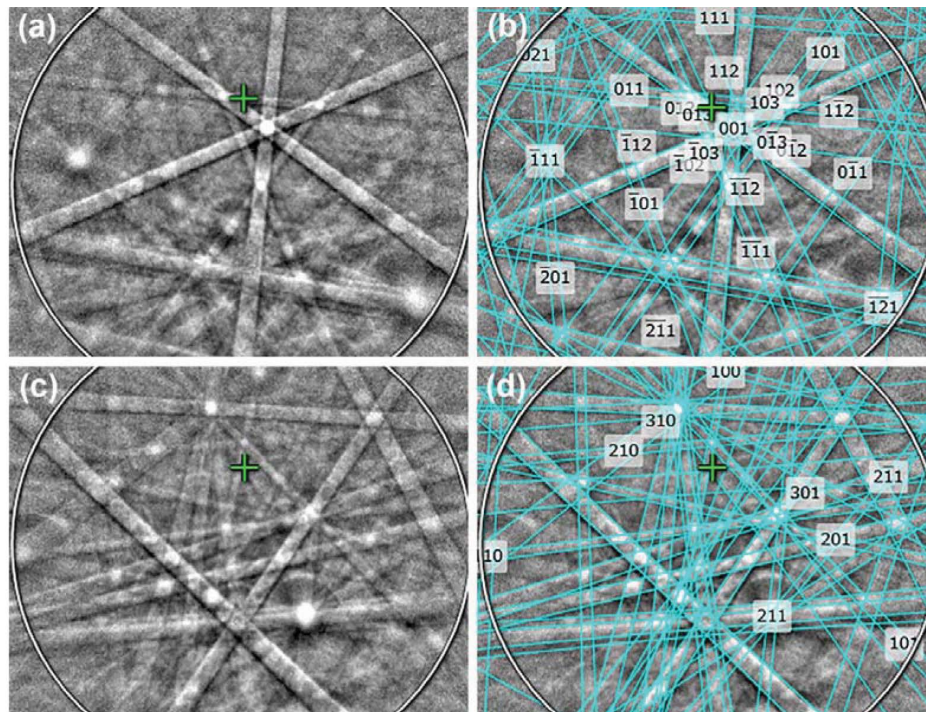**FIGURE 5.** EBSD patterns of armalcolite indexed with the pseudobrookite *Bbmm* structure (MAD = 0.26–0.41). (Color online.)

Figure 6. EBSD patterns of the "Cr-Zr-Ca armalcolite" indexed with the loveringite $R\bar{3}$ structure (MAD = 0.22–0.26). (Color online.)
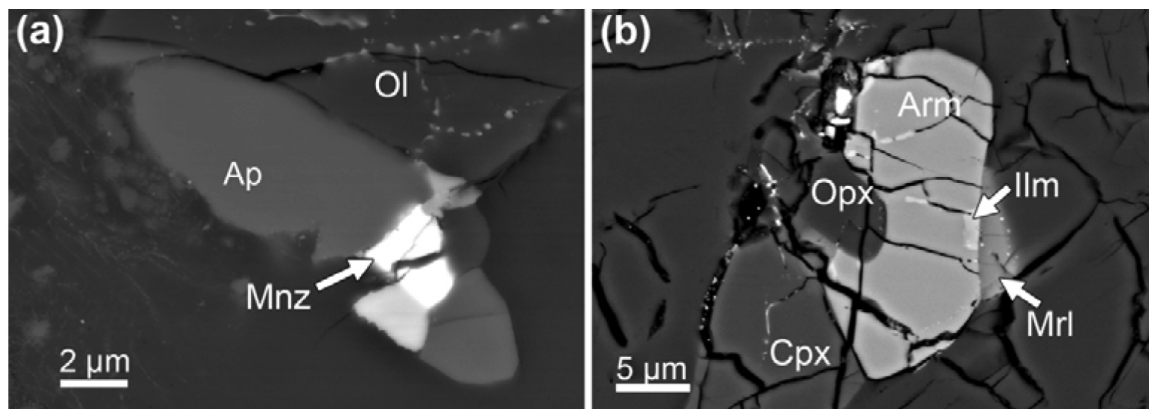
Figure 7. BSE images of phosphate minerals in the Clast-20. (**a**) Fluorapatite and monazite; (**b**) armalcolite and merrillite. Ol = olivine; Opx = orthopyroxene; Cpx = high-Ca pyroxene; Ilm = ilmenite; Ap = apatite; Mrl = merrillite; Mnz = Monazite; Arm = armalcolite.

armalcolite" is $(Ca_{0.99}Na_{0.01})_{\Sigma1.00}(Ti_{14.22}Fe_{2.06}Cr_{2.01}Mg_{1.20}Zr_{0.54}Al_{0.49}Ca_{0.21}Y_{0.05}Mn_{0.04}Ce_{0.03}Si_{0.03}La_{0.01}Nd_{0.01}Dy_{0.01})_{\Sigma20.91}O_{38}$. According to the equation derived from synthetic loveringite by Peterson et al. (1998), the estimated hexagonal cell parameters ***a*** and ***c*** are 10.55 and 20.85 Å, respectively. The ilmenite grains in Clast-20 have high MgO contents (10.9 wt%) with an Mg# value of 0.39. The chromite grains exhibit variations in the contents of Al_2O_3 (17.6–25.8 wt%), Cr_2O_3 (42.7–48.8 wt%), MgO (9.5–10.7 wt%), and FeO (19.7–21.5 wt%). Their Mg# values are in the range of 0.44–0.50. In Clast-20, monazite is also observed besides fluorapatite and merrillite (Figs. 7 and 8). In addition, FeNi metal and Fe-sulfide occur as short veinlets in fractures in silicate minerals or at grain boundaries.

DISCUSSION

EBSD is a bulk electron diffraction technique with high spatial resolution. Therefore, it is a reliable technique for phase identification when combined with compositional analysis (e.g., Michael 2000; El-Dasher and Deal 2009) and has been extensively applied for phase identifications of planetary materials (e.g., Kimura et al. 2009; Ma and Rossman 2009; Zhang et al. 2015; Pang et al. 2016; Chen et al. 2019). In the current study, armalcolite and "Cr-Zr-Ca armalcolite" have different EBSD patterns, which are indexed with two different crystal structures (Figs. 5 and 6). Armalcolite is orthorhombic with a *Bbmm* space group, whereas "Cr-Zr-Ca armalcolite" is hexagonal with a $R\bar{3}$ space group. Therefore, "Cr-Zr-Ca armalcolite" does not belong
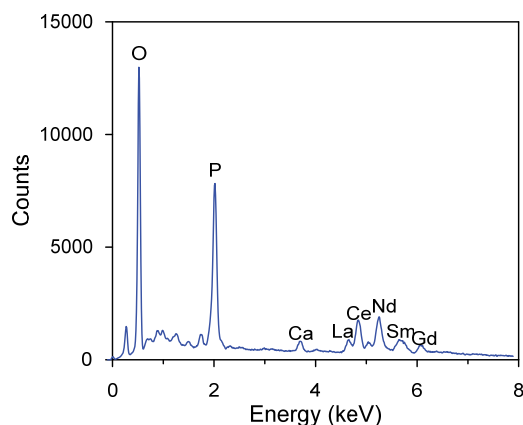
FIGURE 8. SEM-EDS result of the monazite grain shown in Figure 7a. (Color online.)

to the armalcolite family. The EBSD results also exclude the possibility that "Cr-Zr-Ca armalcolite" has the magnetoplumbite structure (Săbău and Alberico 2007). Instead, the low MAD values of the "Cr-Zr-Ca armalcolite" EBSD pattern indexed with the loveringite space group $R\overline{3}$ indicates that the structure of "Cr-Zr-Ca armalcolite" is perfectly consistent with loveringite (Fig. 6). The "Cr-Zr-Ca armalcolite" in Clast-20 also has a chemical formula generally consistent with loveringite. Therefore, the "Cr-Zr-Ca armalcolite" in Clast-20 should be loveringite.

"Cr-Zr-Ca armalcolite" has been reported in mission-returned lunar samples and lunar meteorite (Steele and Smith 1972; Peckett et al. 1972; Haggerty 1972, 1973; Reid et al. 1973; Steele 1974; Treiman and Gross 2015). Most of these lunar "Cr-Zr-Ca armalcolite" data are comparable to those of the "Cr-Zr-Ca armalcolite" in Clast-20, especially for the Cr_2O_3, ZrO_2, and CaO contents (4.3–11.5, 3.6–6.7, and 3.0–4.0 wt%, respectively; Table 3). On the basis of 38 oxygen atoms, the cation sum of these "Cr-Zr-Ca armalcolite" is between 21 and 22, which is similar to that for loveringite (Campbell and Kelly 1978; Gatehouse et al. 1978). The similar chemical compositions suggest that these "Cr-Zr-Ca armalcolite" grains in lunar samples should be loveringite.

An important chemical feature for loveringite in this study is the "excess" of large cations (e.g., Ca, Na, and REE). The ideal formula of loveringite, a member of the crichtonite-group minerals, is $AM_{21}O_{38}$, where A represents the sites for Ca and other large cations, and M represents the sites for small cations. It was thought that the amount of large cations (e.g., Ca, Na, K, Ba, Sr, Pb, and REE) should not be in excess of 1.0 in loveringite and other members of the crichtonite-group minerals (e.g., Haggerty 1983; Haggerty et al. 1983; Săbău and Alberico 2007). However, later investigations demonstrate that Ca in excess of 1 atoms per formula unit (apfu) can incorporate into the largest octahedral site in the loveringite structure based on Rietveld analyses of X-ray diffraction data (Gatehouse and Grey 1983; Gatehouse et al. 1983; Peterson et al. 1998). In this study, we also attribute the Ca in excess of 1 apfu to the largest octahedral site in the loveringite structure, following Peterson et al. (1998).

Zr-armalcolite, which contains much lower contents of Cr_2O_3

and CaO compared with "Cr-Zr-Ca armalcolite," has also been reported in some Apollo samples (e.g., Haggerty 1973; Steele 1974). The Zr-armalcolite data reported by Haggerty (1973) and Steele (1974) have chemical formula more consistent with armalcolite with ideal stoichiometry (3 cations for 5 oxygen atoms). If they are recalculated based on 38 oxygen atoms, the sum of cations would be higher than 22.6 apfu, which is much larger than the stoichiometric cations sum (22 apfu) in loveringite. Therefore, Zr-armalcolite might not be loveringite based on the compositions. However, whether Zr-armalcolite belongs to the armalcolite family remains an open question and requires structural identification in the future.

Loveringite has been reported in many terrestrial samples (Campbell and Kelly 1978; Gatehouse et al. 1978; Haggerty 1983; Lorand et al. 1987; Tarkian and Mutanen 1987; Cabella et al. 1997; Kalfoun et al. 2002; Renna and Tribuzio 2011; Almeida et al. 2014; Rezvukhin et al. 2018) and in a chondrule from the Allende carbonaceous chondrite (Ma et al. 2013). Combining with those in the lunar samples, loveringite may have a large chemical variation from different occurrences. For instance, the variation of the Cr_2O_3 content in loveringite from different locations could be as much as 10 wt% (Haggerty 1973; Campbell and Kelly 1978; Peckett et al. 1972; Almeida et al. 2014). In addition, although most loveringite grains contain a few weight percent of ZrO_2, the loveringite from the Allende chondrite contains only 0.15 wt% ZrO_2 (mean value, Ma et al. 2013). This indicates that ZrO_2 may not be a necessary component in loveringite. Interestingly, many loveringite grains reported in the literature contain rare earth elements (REE) up to a few oxide weight percent (e.g., Campbell and Kelly 1978; Gatehouse et al. 1978), although some of them contain only hundreds to thousands of parts per million of REE (e.g., Haggerty 1983; Lorand et al. 1987; Cabella et al. 1997; Rezvukhin et al. 2018; this study). This indicates that loveringite could be an important carrier of rare earth elements (Green and Pearson 1987) or a proxy of REE-enrichment in the host rocks. Our study shows that the loveringite grains in Clast-20 contain total REE up to 0.9 wt% (Table 3), supporting this inference. Meanwhile, the presence of two REE-rich phosphate minerals monazite and merrillite indicates that Clast-20 should have derived from a REE-rich rock, which supports that loveringite could be a proxy of REE-enrichment.

Many high-Ca pyroxene and low-Ca pyroxene in Clast-20 form an intergrowth texture (Figs. 2–3) that is probably related to exsolution during thermal metamorphism. Based on the compositions of low-Ca and high-Ca pyroxenes, a two pyroxene equilibrium temperature of 1027–1034 °C is derived using different calculation methods (Wells 1977; Brey and Kohler 1990). Considering the potential effect of $NaCrSi_2O_6$ component, the mean temperature of clinopyroxene for Clast-20 is 959 ± 53 °C (Nakamuta et al. 2017), slightly lower than the temperatures from the two-pyroxene thermometry. Although the presence of glassy plagioclase and veinlet-like FeNi metal and Fe-sulfide grains indicates that Clast-20 was subjected to a shock metamorphism, no evidence implies that the shock event had disturbed the equilibrium between low-Ca and high-Ca pyroxenes. Therefore, the high equilibrium temperature may imply that the source rock of Clast-20 is a plutonic rock. This is consistent with the fact that most terrestrial loveringite grains

were usually observed in intrusions or mantle rocks (Campbell and Kelly 1978; Gatehouse et al. 1978; Lorand et al. 1987; Tarkian and Mutanen 1987; Cabella et al. 1997; Kalfoun et al. 2002; Renna and Tribuzio 2011; Almeida et al. 2014). The tiny ilmenite inclusions in armalcolite might be the exsolution products during the same thermal metamorphic event.

"Cr-Zr-Ca armalcolite" (loveringite) in mission-returned lunar samples was mainly described from Apollo samples and Luna soils. However, unfortunately, their petrographic textures were not always described clearly, which makes direct comparison of loveringite's host rocks difficult. In lunar meteorites, it was only reported in a magnesian suite lithic clast (Clast U) in the feldspathic lunar breccia ALHA81005 (Treiman and Drake 1983; Treiman and Gross 2015). Combining all the information together, most of the mafic silicate minerals that are associated with loveringite (including this study) have high Mg# values, although loveringite does not have a high Mg# value. This indicates that the source rocks of lunar loveringite might be magnesian suite rocks (e.g., Steele and Smith 1972; Steele 1974; Treiman and Gross 2015). The high MgO content in ilmenite that is associated with loveringite also supports this inference (Steele 1974). This provides an opportunity to understand the diversity of magnesian suite rocks in lunar samples (Treiman and Gross 2015).

The Clast-20 in this study has many features similar to the Clast U in ALHA81005 described by Treiman and Gross (2015). For instance, both clasts have similar mineral assemblages that contain olivine, plagioclase, low-Ca pyroxene, high-Ca pyroxene, chromite, ilmenite, loveringite, rutile, and Ca-phosphate minerals, although clast-20 in this study also contains armalcolite and monazite as accessory minerals. The contents and variations of minor elements (e.g., TiO_2 and Cr_2O_3) in the pyroxenes from both clasts are also generally similar (Treiman and Gross 2015; this study). The similarities in mineral assemblage and mineral chemistry indicate that they might have similar source rocks. The presence of both Ca-phosphate minerals and loveringite implies that their source rocks are rich in phosphorus and rare earth elements. However, there are two important differences between Clast-20 and Clast U. First, the mafic silicate minerals in Clast-20 have higher Mg# values (0.86–0.91) than those in Clast U (0.79–0.83, Treiman and Gross 2015). This implies that Clast-20 is more primitive (less fractionated) than Clast U. Second, the pyroxene grains in Clast U show a large chemical zoning (Treiman and Gross 2015), which was not observed in Clast-20 in this study. This difference probably reflects different crystallization and/or metamorphic histories.

Treiman and Gross (2015) compared Clast U with other magnesian suite rocks. They found that Clast U is unique in mineral assemblage and mineral chemistry. The similarity in mineral assemblage and mineral chemistry between Clast-20 and Clast U implies that Clast-20 is also very unique compared to mission-returned magnesian suite rocks and magnesian suite lithic clasts in most lunar meteorites. Considering the An value of plagioclase and the Mg# values of mafic silicate minerals, Clast-20 will plot outside of the regions for magnesian suite rocks (Fig. 1 of Treiman and Gross 2015), supporting the claim by Treiman and Gross (2015) that the magnesian suite rocks may be more diverse than apparent in the Apollo samples.

IMPLICATIONS

The Clast-20 in NWA 8182 provides an important sample to solve the puzzle of whether the "Cr-Zr-Ca armalcolite" belongs to the armalcolite family. Our EPMA and EBSD results reveal that "Cr-Zr-Ca armalcolite" is different from armalcolite and is loveringite instead. Owing to the structural characteristic of loveringite in containing large cations, it seems that rare earth elements can be readily incorporated into the loveringite structure. For lunar samples, the presence of loveringite might be an important indicator of REE-enrichment. At the same time, loveringite is only observed in Mg-rich lithologies, no matter from terrestrial or extraterrestrial rocks. Therefore, loveringite is also an important indicator of lunar Mg-suite rocks. The high Mg# values of mafic silicate minerals and the enrichment of phosphorus and REE in Clast-20 support the inference that some lunar Mg-suite rocks could be related to KREEPy lithologies, although Mg-suite magmas are not required to have a KREEP signature (Shearer et al. 2015). However, although the Clast-20 is an Mg-suite lithic clast, the chemical compositions of its mafic silicate minerals and plagioclase are different from those in other Mg-suite rocks in Apollo samples and lunar meteorites. This indicates that Clast-20 represents a new example of diverse lunar Mg-suite rocks.

REFERENCES CITED

Almeida, V.V., Janasi, V. de, A., Svisero, D.P., and Nannini, F. (2014) Mathiasite-loveringite and priderite in mantle xenoliths from the Alto Paranaiba igneous province, Brazil: genesis and constraints on mantle metasomatism. Central European Journal of Geosciences, 6, 614–632.

Anderson, A.T., Bunch, T.E., Cameron, E.N., Haggerty, S.E., Boyd, F.R., Finger, L.W., James, O.B., Keil, K., Prinz, M., Ramdohr, P., and El Goresy, A. (1970) Armalcolite: a new mineral from the Apollo 11 samples. Proceedings of the Apollo 11 Lunar Science Conference, 1, 55–63.

Brey, G.P., and Kohler, T. (1990) Geothermobarometry in four-phase lherzolites II. New thermobarometers, and practical assessment of existing thermobarometers. Journal of Petrology, 31, 1353–1378.

Cabella, R., Gazzotti, M., and Lucchetti, G. (1997) Loveringite and baddeleyite in layers of chromian spinel from the Bracco ophiolitic unit, northern Apennines, Italy. Canadian Mineralogist, 35, 899–908.

Campbell, I.H., and Kelly, P.R. (1978) Geochemistry of loveringite, a uranium-rare-earth-bearing accessory phase from Jimberlana intrusion of Western Australia. Mineralogical Magazine, 42, 187–193.

Chen, D.L., Zhang, A.C., Pang, R.L., Chen, J.N., and Li, Y. (2019) Shock-induced phase transformation of anorthitic plagioclase in the eucrite meteorite Northwest Africa 2650. Meteoritics & Planetary Science, 54, 1548–1562.

Contini, S., Venturelli, G., and Toscani, L. (1993) Cr-Zr-armalcolite-bearing lamproites of Cancarix, SE Spain. Mineralogical Magazine, 57, 203–216.

El-Dasher, B., and Deal, A. (2009) Application of electron backscatter diffraction to phase identification. In A.J. Schwartz, M. Kumar, B.L. Adams, and D.P. Field, Eds., Electron Backscatter Diffraction in Materials Science, 2nd ed., p. 81–96. Springer.

Gatehouse, B.M., and Grey, I.E. (1983) The crystal structure of $Ca_2Zn_4Ti_{16}O_{38}$. Journal of Solid State Chemistry, 46, 151–155.

Gatehouse, B.M., Grey, I.E., Campbell, I.H., and Kelly, P. (1978) The crystal structure of loveringite—a new member of the crichtonite group. American Mineralogist, 63, 28–36.

Gatehouse, B.M., Grey, I.E., and Smyth, J.R. (1983) Structure refinement of mathiasite, $(K_{0.62}Na_{0.14}Ba_{0.14}Sr_{0.10})_{\Sigma1.0}[Ti_{12.90}Cr_{3.10}Mg_{1.53}Fe_{2.15}Zr_{0.67}Ca_{0.29}(V,Nb,Al)_{0.36}]_{\Sigma21.0}O_{38}$. Acta Crystallographica, C39, 421–422.

Green, T.H., and Pearson, N.J. (1987) High-pressure, synthetic loveringite-davidite

and its rare-earth element geochemistry. Mineralogical Magazine, 51, 145–149.

Grégoire, M., Lorand, J.P., O'Reilly, S.Y., and Cottin, J.Y. (2000) Armalcolite-bearing, Ti-rich metasomatic assemblages in harzburgitic xenoliths from the Kerguelen Islands: Implications for the oceanic mantle budget of high-field strength elements. Geochimica et Cosmochimica Acta, 64, 673–694.

Haggerty, S.E. (1972) The mineral chemistry of some decomposition and reaction assemblages associated with Cr-Zr, Ca-Zr, and Fe-Mg-Zr titanates. In J.W. Chamberlain and C. Watkins, Eds., The Apollo 15 Lunar Samples, p. 88–91. The Lunar Science Institute.

——— (1973) Armalcolite and genetically associated opaque minerals in the lunar samples. Proceedings of the Fourth Lunar Science Conference, 777–797.

——— (1983) The mineral chemistry of new titanates from the Jagersfontein Kimberlite, South Africa: Implications for metasomatism in the upper mantle. Geochimica et Cosmochimica Acta, 47, 1833–1854.

Haggerty, S.E., Smyth, J.R., Erlank, A.J., Rickard, R.S., and Danchin, R.V. (1983) Lindsleyite (Ba) and mathiasite (K): two new chromium-titanates in the crichtonite series from the upper mantle. American Mineralogist, 68, 494–505.

Heiken, G.H., Vaniman, D.T., and French, B.M. (1991) Lunar Sourcebook: A User's Guide to the Moon, p. 721. Cambridge University Press.

Jolliff, B.L., Wieczorek, M.A., Shearer, C.K., and Neal, C.R. (2006) New Views of the Moon, vol. 60, 721 p. Reviews in Mineralogy and Geochemistry, Mineralogical Society of America, Chantilly, Virginia.

Kalfoun, F., Ionov, D., and Merlet, C. (2002) HFSE residence and Nb/Ta ratios in metasomatized, rutile-bearing mantle peridotites. Earth and Planetary Science Letters, 199, 49–65.

Lattard, D. (1987) Subsolidus phase relations in the system Zr-Fe-Ti-O in equilibrium with metallic iron. Implications for lunar petrology. Contributions to Mineralogy and Petrology, 97, 264–278.

Levy, C., Christophe-Michel-Levy, M., Picot, P., and Caye, R. (1972) A new titanium and zirconium oxide from the Apollo 14 samples. Proceedings of the Third Lunar Science conference. Geochimica et Cosmochimica Acta, Suppl. 3, 1115–1120.

Lorand, J.P., Cottin, J.Y., and Parodi, G.C. (1987) Occurrence and petrological significance of loveringite in the Western Laouni layered complex, southern Hoggar, Algeria. Canadian Mineralogist, 25, 683–693.

Kimura, M., Mikouchi, T., Suzuki, A., Miyahara, M., Ohtani, E., and El Goresy, A. (2009) Kushiroite, CaAlAlSiO$_6$: A new mineral of the pyroxene group from the ALH 85085 CH chondrite, and its genetic significance in refractory inclusions. American Mineralogist, 94, 1479–1482.

Ma, C., and Rossman, G.R. (2009) Tistarite, Ti$_2$O$_3$, a new refractory mineral from the Allende meteorite. American Mineralogist, 94, 841–844.

Ma, C., Beckett, J.R., Connolly, H.C., Jr., and Rossman, G.R. (2013) Discovery of meteoritic loveringite, Ca(Ti,Fe,Cr,Mg)$_{21}$O$_{38}$, in an Allende chondrule: late stage crystallization in a melt droplet. 44th Lunar and Planetary Science Conference, Abstract 1443.

Michael, J.R. (2000) Phase identification using electron backscatter diffraction in the scanning electron microscope. In A.J. Schwartz, M. Kumar, and B.L. Adams, Eds., Electron Backscatter Diffraction in Materials Science, p. 75–90. Kluwer.

Nakamuta, Y., Urata, K., Shibata, Y., and Kuwahara, Y. (2017) Effect of NaCrSi$_2$O$_6$ component on Lindsley's pyroxene thermometer: An evaluation based on strongly metamorphosed LL chondrites. Meteoritics & Planetary Science, 52, 511–521.

Pang, R.L., Zhang, A.C., Wang, S.Z., Wang, R.C., and Yurimoto, H. (2016) High-pressure minerals in eucrite suggest a small source crater on Vesta. Scientific Reports, 6, 26063.

Papike, J.J., Ryder, G., and Shearer, C.K. (1998) Lunar samples. In J.J. Papike, Ed., Planetary Materials, vol. 36, p. 5.1–5.234. Reviews in Mineralogy, Mineralogical Society of America, Chantilly, Virgnia.

Peckett, A., Phillips, R., and Brown, G.M. (1972) New zirconium-rich minerals from Apollo 14 and 15 lunar rocks. Nature, 236, 215–217.

Peterson, R.C., Grey, I.E., Cranswick, L.M.D., and Li, C. (1998) The stability and crystal chemistry of synthetic loveringite in the system Ca-Mn-Ti-O under strongly reducing conditions. The Canadian Mineralogist, 36, 763–774.

Reid, A.M., Warner, J.L., Ridley, W.I., and Brown, R.W. (1973) Lunar 20 soil: abundance and composition of phases in the 45–125 micron fraction. Geochimica et Cosmochimica Acta, 37, 1011–1030.

Renna, M.R., and Tribuzio, R. (2011) Olivine-rich troctolites from Ligurian Ophiolites (Italy): Evidence for impregnation of replacive mantle conduits by MORB-type melts. Journal of Petrology, 52, 1763–1790.

Rezvukhin, D.I., Malkovets, V.G., Sharygin, I.S., Tretiakova, I.G., Griffin, W.L., and O'Reilly, S.Y. (2018) Inclusions of crichtonite-group minerals in Cr-pyropes from the Internatsionalnaya kimberlite pipe, Siberian Craton: Crystal chemistry, parageneses and relationships to mantle metasomatism. Lithos, 308-309, 181–195.

Săbău, G., and Alberico, A. (2007) What is CCZN-armalcolite? A crystal-chemical discussion and an ad-hoc incursion in the crichtonite-minerals group. Studia Universitatis Babes-Bolyai, Geologia, 52, 55–66.

Schulze, D.J. (1990) Silicate-bearing rutile-dominated nodules from South Africa Kimberlites: Metasomatized cumulates. American Mineralogist, 75, 97–104.

Shearer, C.L., Elardo, S.M., Petro, N.E., Borg, L.E., and McCubbin, F.M. (2015) Origin of the lunar highlands Mg-suite: An integrated petrology, geochemistry, chronology, and remote sensing perspective. American Mineralogist, 100, 294–325.

Steele, I.M. (1974) Ilmenite and armalcolite in Apollo 17 Breccias. American Mineralogist, 59, 681–689.

Steele, I.M., and Smith, J.V. (1972) Occurrence of diopside and Cr-Zr-armalcolite on the Moon. Nature Physical Science, 237, 105–106.

Tarkian, M., and Mutanen, T. (1987) Loveringite from the Koitelainen layered intrusion, Northern Finland. Mineralogy and Petrology, 37, 37–50.

Treiman, A.H., and Drake, M.J. (1983) Origin of lunar meteorite ALHA81005: Clues from the presence of terrae clasts and a very low-titanium mare basalt clasts. Geophysical Research Letters, 10, 783–786.

Treiman, A.H., and Gross, J. (2015) A rock fragment related to the magnesian suite in lunar meteorite Allan Hills (ALHA) 81005. American Mineralogist, 100, 441–446.

Wechsler, B.A. (1977) Cation distribution and high-temperature crystal chemistry of armalcolite. American Mineralogist, 62, 913–920.

Wells, P.R.A. (1977) Pyroxene thermometry in simple and complex systems. Contributions to Mineralogy and Petrology, 62, 129–139.

Zhang, A.C., Ma, C., Sakamoto, N., Wang, R.C., Hsu, W.B., and Yurimoto, H. (2015) Mineralogical anatomy and implications of a Ti-Sc-rich ultrarefractory inclusion from Sayh al Uhaymir 290 CH3 chondrite. Geochimica et Cosmochimica Acta, 163, 27–39.